

# Hydroelectric System Response to Part Load Vortex Rope Excitation

S Alligné<sup>1</sup>, C Nicolet<sup>1</sup>, A Béguin<sup>1</sup>, C Landry<sup>2</sup>, J Gomes<sup>2</sup>, F Avellan<sup>2</sup>

<sup>1</sup> Power Vision Engineering Sàrl, Ch. Des champs courbes 1, CH 1024 Ecublens, Switzerland

<sup>2</sup> Ecole Polytechnique Fédérale de Lausanne, Laboratory for Hydraulic Machines, CH 1007 Lausanne, Switzerland

**Abstract.** The prediction of pressure and output power fluctuations amplitudes on Francis turbine prototype is a challenge for hydro-equipment industry since it is subjected to guarantees to ensure smooth and reliable operation of the hydro units. The European FP7 research project Hyperbole aims to setup a methodology to transpose the pressure fluctuations induced by the cavitation vortex rope on the reduced scale model to the prototype generating units. A Francis turbine unit of 444MW with a specific speed value of  $v = 0.29$ , is considered as case study. A SIMSEN model of the power station including electrical system, controllers, rotating train and hydraulic system with transposed draft tube excitation sources is setup. Based on this model, a frequency analysis of the hydroelectric system is performed to analyse potential interactions between hydraulic excitation sources and electrical components.

## 1. Introduction

Due to the development of renewable energy and modification of electricity market, the extension of the operating range of hydraulic machines to off-design conditions is more and more requested by power utilities, but the prediction of the related pressure and output power fluctuations remains a challenging task [1-8]. In the framework of the European FP7 research project Hyperbole, a methodology is setup to predict pressure and output power fluctuations on prototype induced by the cavitation vortex rope based on experimental measurements on the reduced scale model. The developed methodology relies on an advanced modelling of the draft tube cavitation flow which main parameters are the cavitation compliance, the dissipation and the excitation source [9]. Specific measurements to quantify this dissipation with the remaining parameters are required [10]. First, this paper presents the methodology and focus on the transposition to the prototype of the draft tube model parameters identified on the reduced scale model. Then, a numerical model of the power station including electrical system, controllers, rotating train and hydraulic system with transposed draft tube excitation sources is setup. Based on this model, frequency response [11] of the electro-mechanical, the hydro-mechanical and the hydroelectric systems are compared to analyse the influence of the different modelling approaches to predict both pressure and output power fluctuations induced by the cavitation vortex.

## 2. Methodology

### 2.1. Overview

The methodology to predict the pressure fluctuations on prototype is illustrated in figure 1. The first step is to identify the hydroacoustic characteristics of the draft tube cavitation vortex rope on a Francis turbine reduced scale model installed on a test rig. To achieve this, the test rig hydraulic circuit is excited by an external periodical discharge source and the system response is compared to the response of a numerical model of the test rig [10]. An identification process comparing experimental and numerical hydraulic responses enables to identify the parameters of an advanced model of the draft tube cavitation flow. Then, these reduced scale model parameters are transposed to the prototype and used in the numerical model of the actual power plant for the prediction of the resulting pressure fluctuations. This paper presents the second step of the methodology and is focused on the transposition at part load conditions.

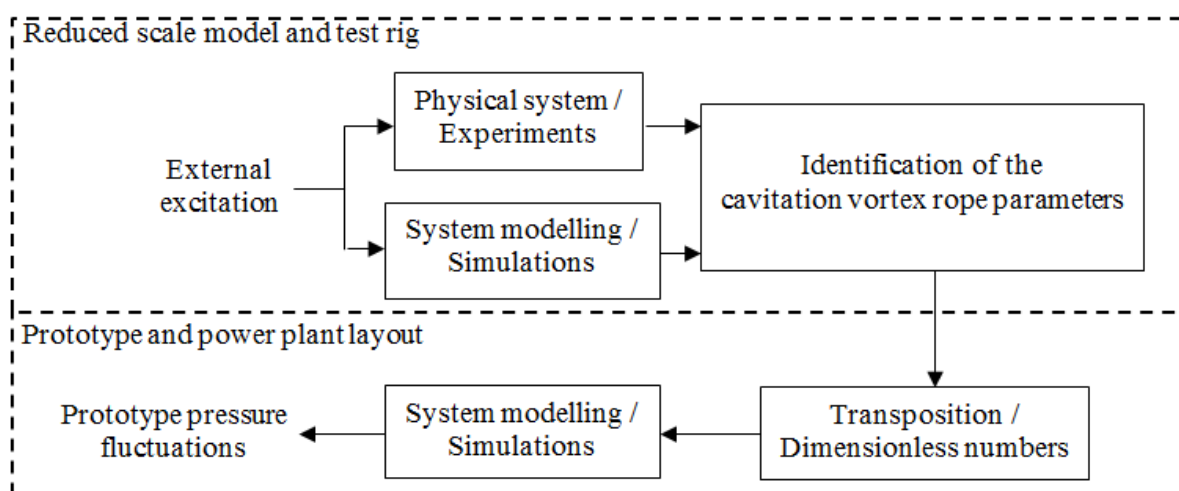


**Figure 1.** Methodology for prediction of pressure fluctuations on prototype.

### 2.2. Modelling of the reduced scale model draft tube

The modelling of the draft tube cavitation flow is described by continuity and momentum equations (1) and (2) including the convective terms and the divergent geometry [9].

$$dQ = -\frac{dV_c}{dt} = C_c \frac{dh}{dt} + \chi \frac{dQ}{dt} \quad (1)$$

$$\frac{1}{gA} \frac{\partial Q}{\partial t} + \frac{Q}{gA^2} \frac{\partial Q}{\partial x} - \frac{Q^2}{gA^3} K_x + \frac{\partial h}{\partial x} + \frac{\tau_0 \pi D}{\rho g A} - \frac{\mu''}{\rho g A} \frac{\partial^2 Q}{\partial x^2} + S_h = 0 \quad (2)$$

For this investigation, three cavitation vortex rope parameters of this model have been identified experimentally at the reduced scale model:

- the local wave speed  $a$  defined implicitly by the cavitation compliance  $C_c$  (the mass flow gain factor  $\chi$  is not considered in this study);
- the second viscosity  $\mu''$  introducing dissipation induced by the phase change during cavitation volume fluctuations;
- the momentum excitation source  $S_h$  induced by the helical swirling flow.

### 2.3. Dimensionless numbers and transposition law

By applying the Buckingham -  $\Pi$  theorem, the wave speed and the second viscosity are normalized by the outlet pressure level of the draft tube, leading to two dimensionless numbers, see equation (3).

These dimensionless numbers can be approximated by a power function of the void fraction  $\beta$  which are not dependent on the operating point of the hydraulic machine in the range of part load conditions [10].

$$\Pi = \frac{\rho_w a^2}{P_{out} - P_v} = g(\beta) \quad ; \quad M^* = \frac{\mu^n f_{natural}}{P_{out} - P_v} = \Pi^2 (1 - \beta^2) \frac{\rho_c}{\rho_w} \quad (3)$$

To use these dimensionless numbers the void fraction  $\beta$  must be known and is derived from a cavitation curve  $\beta = f(\sigma)$  depending on the operating point and the Froude number. By assuming the Froude similitude the prototype void fraction  $\beta^P$  is equal to the reduced scale model void fraction  $\beta^M$ .

### 3. Hydraulic layout modelling of the power plant

#### 3.1. General characteristics

The power plant of interest features four 435MW generating units, each equipped with a Francis type turbine rated at power output of 444 MW under the 171m rated net head. The main characteristics of the hydro units are given in table 1a). Each unit is supplied by individual power conduits including intake, penstock and draft tube. The length of each penstock is about 310 meters. The draft tube model parameters at reduced scale model have been derived for two part load operating points named PL1 and PL2, given in table 1b).

**Table 1.** a) Hydro unit characteristics and b) Investigated operating points.

a)			b)			
Pm	(MW)	444		PL1	PL2	
H	(m)	171	GVO	(°)	15	12
N	(rpm)	128.6	nED / nED BEP	(-)	1	1
v	(-)	0.29	QED / QED BEP	(-)	0.8	0.64
			Fr	(-)	5.6	5.6
			$\sigma$	(-)	0.11	0.11

#### 3.2. Transposed draft tube model parameters

A numerical model of the power plant is set up with the SIMSEN software including reservoirs, penstock, the two quadrant characteristic of the turbine, the rotating inertia and the advanced cavitation draft tube model. The draft tube is divided in two parts: one from the outlet runner to the middle of the elbow where cavitation is developed and the other one down to the outlet draft tube, which is cavitation free, by defining an equivalent cross sectional area of the two channels after the peer, see figure2.

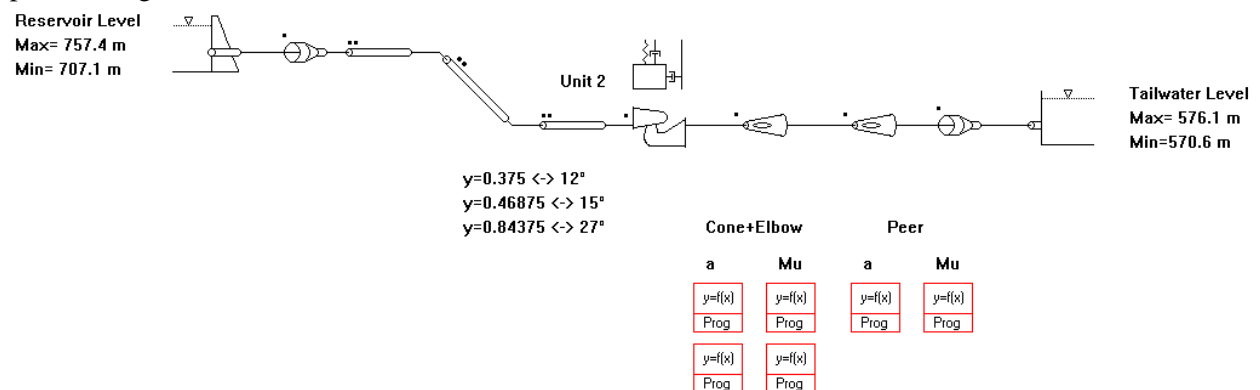


**Figure 2.** SIMSEN hydro-mechanical model

In the draft tube part with cavitation, a distributed model is used. It is characterized by several control volumes along the draft tube length where equations (1) and (2) are applied. Constant wave speed and second viscosity parameters are considered along the draft tube length [12]. Table 2 shows the influence of the operating point on the transposed prototype draft tube parameters and on the resulting first eigenmodes of the power plant defined by frequency and damping  $s = \alpha + j(2\pi f)$ . By changing the operating point from PL1 to PL2, the void fraction is increased. Hence, the first eigenfrequency value  $f_1$  is decreased from 0.30 to 0.18 times the runner frequency  $n$  and the eigendamping value  $\alpha_1$  is increased towards positive values.

**Table 2.** Influence of the operating point on the draft tube parameters and on the resulting three first eigenfrequencies.

	PL1	PL2
$\sigma$ (-)	0.11	0.11
$\beta$ (-)	0.0124	0.0421
$a$ (m/s)	76.9	45.3
$\mu''$ (Pa.s)	3.06E+05	6.14E+04
$\alpha_1$ ( $s^{-1}$ )	-0.40	-0.10
$f_1/n$ (-)	0.30	0.18
$\alpha_2$ ( $s^{-1}$ )	-0.86	-1.02
$f_2/n$ (-)	0.78	0.69
$\alpha_3$ ( $s^{-1}$ )	-6.67	-1.09
$f_3/n$ (-)	1.05	0.80

#### 4. Electrical layout modelling of the power plant

Figure 3 shows the SIMSEN model of the electrical systems of one generation unit of the power plant. This model contains the grid access point, the unit's step-up transformer, the electrical machine and its excitation system.

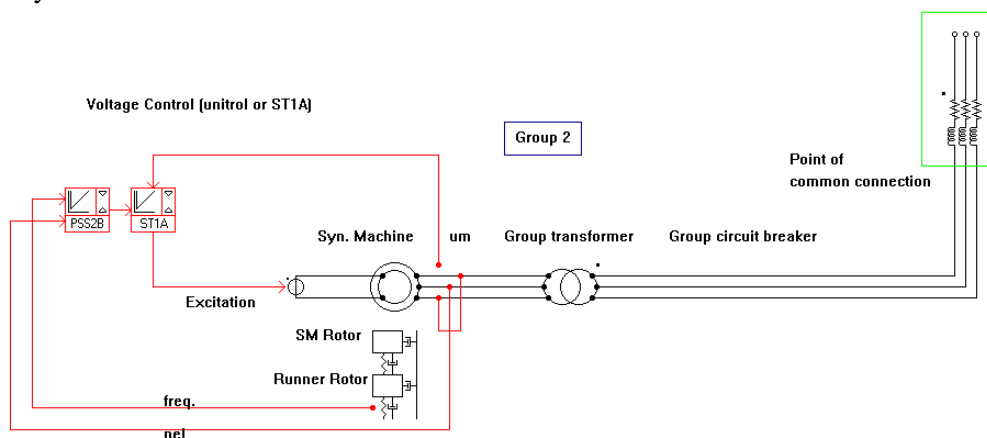


**Figure 3.** SIMSEN electro-mechanical model

##### 4.1. Electrical grid

The connection to the grid is modelled with an infinite power three phase voltage bus behind a short-circuit impedance, to represent the short-circuit power limitation of the connection point. Nominal voltage of grid is 500 kV and short circuit power is about 9 times the nominal power of the unit and with X/R ratio of about 25. The rather low short-circuit power is due to a long transmission line. In reality, this line is installed with series capacitors and shunt reactors for compensation of its reactive power consumptions. This has been neglected in order to focus on the power plant itself.

#### 4.2. Electrical machine

The electrical machine is a synchronous machine with salient poles which nominal values are given in table 3. The model used for such machine is a 6th order model consisting in an equivalent circuit for the direct (d) and quadrature (q) axis. This model has the windings voltage equations for the three stator windings, the excitation winding and two damper windings, one for each d and q axis.

**Table 3.** Synchronous machine nominal values

$S_n$	(MVA)	526
$U_n$	(kV)	16
$F_n$	(Hz)	60
$P_p$	(-)	28

#### 4.3. Excitation system

The excitation systems consist in a static exciter and a voltage controller both represented by the IEEE ST1A excitation model. Besides, the excitation system is equipped with a power system stabilizer (PSS) represented by a IEEE PSS2B PSS model.

### 5. Frequency analysis of the hydroelectric powerplant

To characterize the dynamic system response in the frequency domain, transfer functions are computed by performing a time domain simulation with a white noise excitation modelled by a Pseudo Random Binary Sequence (PRBS) [11] considering two different types of excitations:

- a momentum excitation source in the draft tube for the hydro-mechanical and the hydroelectric systems
- an external torque on the rotating masses for the electro-mechanical system.

With a period of  $dT = 0.1$  s, the energy spectrum of the PRBS signal is distributed uniformly in the range 0 to 5Hz, covering the excitation range of the helical vortex rope being between 0.2 and 0.4 times the runner frequency  $n$  corresponding respectively to 0.43 Hz and 0.86 Hz.

#### 5.1. Hydro-mechanical and hydroelectric systems

The amplitude of the normalized transfer function of the hydro-mechanical system, defined as the ratio between the draft tube pressure cone and the momentum excitation source in the draft tube, is represented in figure 4 for the two investigated operating points, see equation (5).

$$G(s) = \frac{H_{C_{DT}}(s)/H_n}{S_n(s)/H_n} \quad (5)$$

Due to the higher void fraction for PL2, the second viscosity is lower and therefore, damping values of the eigenmodes and system response amplitude are higher. The vortex rope frequency being between 0.2 and 0.4 times the runner frequency  $n$  (yellow area in figure 4), a matching with the first eigenfrequency is only feasible at PL1 where amplitudes are rather small for resonance conditions. For PL2, the amplitude response obtained for the second eigenmode at this location is higher than the one obtained for PL1 despite a higher damping value  $\alpha$  for PL2. This effect is due to the difference of cavitation parameters between PL1 and PL2 that affects the spatial distribution of pressure amplitudes along the piping system and also to the difference of relative position of the excitation source in the eigenmode.

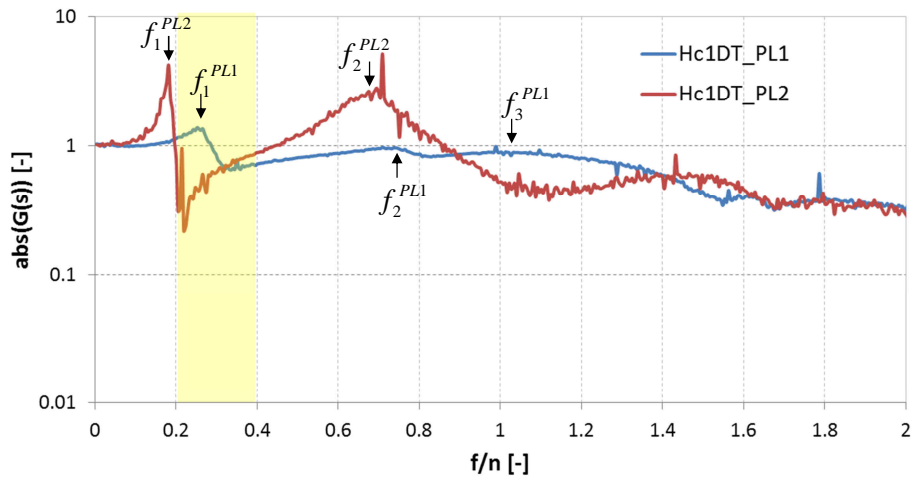


**Figure 4.** Hydro-mechanical system - Amplitude of draft tube pressure cone transfer functions for PL1 and PL2.

In figure 5, a comparison of the draft tube pressure cone transfer functions between hydro-mechanical and hydroelectric system is performed. It is shown that in the low frequency range, the electrical part of the system does not influence the hydraulic response. Hence, modelling electrical system with constant speed is sufficient for prediction of pressure fluctuations for this case. However, results might be different for a weaker power network.

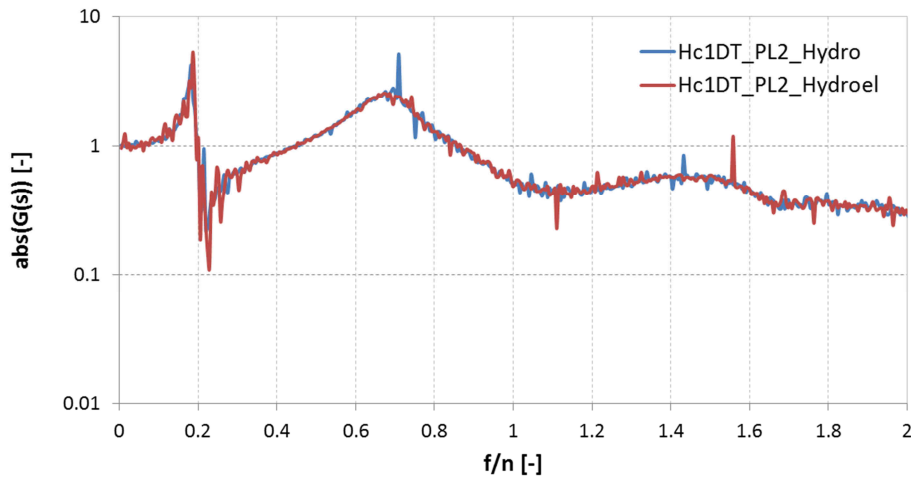


**Figure 5.** Comparison of draft tube pressure cone transfer functions between hydro-mechanical system and hydroelectric system for PL2

### 5.2. Electro-mechanical and hydroelectric systems

In figure 6, the amplitude of the normalized transfer functions defined as the ratio between the output power and the external excitation source are plotted for the three modelling approaches with electro-mechanical, hydro-mechanical and hydroelectric models. These transfer functions are plotted for the two investigated operating points and are defined by equations (6):

$$G(s)_{electro} = \frac{P(s)/P_n}{T_{ext}(s)/T_n} \quad ; \quad G(s)_{hydro} = \frac{P_m(s)/P_n}{S_h(s)/H_n} \quad ; \quad G(s)_{hydroel} = \frac{P(s)/P_n}{S_h(s)/H_n} \quad (6)$$

For electro-mechanical and hydroelectric models the output power is the active power whereas for the hydro-mechanical model, the output power corresponds to the mechanical power.

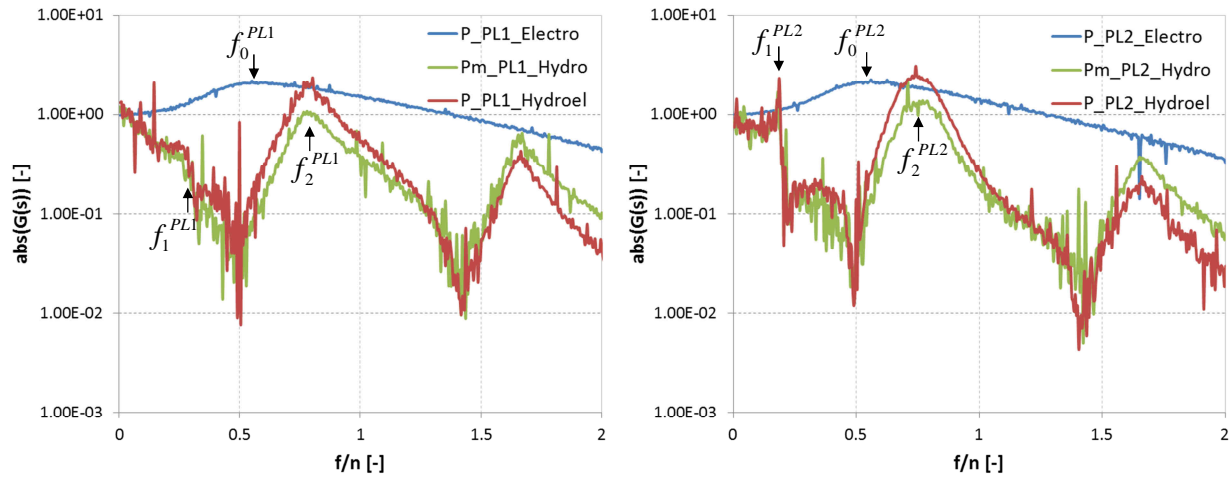


**Figure 6.** Comparison of active power transfer functions between electro-mechanical system and hydroelectric system for PL1 (left) and PL2 (right)

The “local eigenmode” of the synchronous machine representing the rotor oscillations against the power grid is found at 1.2Hz, i.e.  $f_0/n=0.56$  times the runner frequency  $n$ . This mode is clearly observed with the transfer function of the electro-mechanical system. With the hydroelectric model, the transfer function of the active power is influenced by the hydraulic system, since hydraulic eigenfrequencies can be observed. Hence, with an electro-mechanical model, the modelling of the vortex rope excitation source by just an external source torque is not representative of the hydraulic system dynamics. Indeed, hydraulic eigenfrequencies, which may interact with the vortex rope precession frequency, are not transmitted to the power network. It has been shown that the hydroelectric model predicts the same pressure fluctuations in the hydraulic system as the hydro-mechanical model, see figure 5. However, for prediction of output power fluctuations, the modelling of the electrical part is necessary and the hydro-mechanical model is not sufficient anymore. Indeed, the hydroelectrical transfer function is the result of the multiplication between the hydro-mechanical and the electro-mechanical transfer functions. Hence, the transfer function of the electro-mechanical model, featuring the synchronous machine local eigenmode, amplifies or reduces the prediction of the mechanical power fluctuations of the hydro-mechanical model. For the PL2 operating point, this local eigenmode amplifies the second hydraulic eigenfrequency and results in prediction of higher amplitude than the electro-mechanical model.

## 6. Conclusions

The methodology developed in the framework of the European Hyperbole project has been applied to a 435MW generating unit of Francis type turbine. Parameters of the reduced scale draft tube model have been transposed to the prototype for two operating points at part load. These parameters are integrated in a SIMSEN model of the power station including electrical system, controllers, rotating train and hydraulic system. Based on this model setup with the transposed parameters, frequency analysis of the electro-mechanical, the hydro-mechanical and the hydroelectric systems are compared. It has been shown that in the low frequency range, hydro-mechanical models are sufficient for prediction pressure fluctuations in the hydraulic system. This could be different for weaker or isolated power networks. However, for prediction of output power, the hydroelectric model is necessary. Compared to the electro-mechanical model, the detailed hydraulic modelling enables to take into account potential hydraulic resonances and anti-resonances resulting from the interaction of the cavitation vortex rope precession frequency with the hydraulic system that influences potential power fluctuations transmitted to the power network. On the other hand, compared to the hydro-mechanical model, the dynamics of the electrical machine can amplify or reduce the mechanical power fluctuations. Measurements on prototype are foreseen to validate these results.

## 7. References

- [1] Rheingans, W.J., Power swing in hydroelectric power plants. Transactions ASME 62, 1940, pp. 171-184
- [2] Fritsch, A., Maria, D., Comportement dynamique d'une turbine Francis à charge partielle: comparaison modèle-prototype. *La Houille Blanche*, N°3/4, 1988, pp. 273-280.
- [3] Tadel, J., Maria, D., Analysis of dynamic behavior of a hydroelectric installation with Francis turbine. In Proc. 5th Int. Conf. on Pressure Surges, Hannover, Germany, 1986, pp.43-52.
- [4] Jacob, T., Evaluation sur modèle réduit et prédiction de la stabilité de fonctionnement des turbines Francis. Thesis, Lausanne, EPFL, 1993.
- [5] Hell J., Glaninger A., Schürhuber R., Egretzberger M., Interference of parallel operating hydro generating units connected to a weak grid. International conference Hydro 2011, Prague, Czech Republic, 2011.
- [6] Bollinger K.E., Nettleton L.D., Gurney J.H., Reducing the effect of penstock pressure pulsations on hydroelectric plant power system stabilizer signals. IEEE Transactions on Energy Conversion, 1993, Vol. 8, N°4.
- [7] Konidaris D.N., Tegopoulos J.A., Investigation of oscillatory problems of hydraulic generating units equipped with Francis turbines. IEEE Transactions on Energy Conversion, 1997, Vol.12, N°4.
- [8] Gautam, P., Gummer, J.H., Pott, J., Local penstock resonance resulting from turbine operation, In Proc. of the IAHR Symposium, Montréal, 2014.
- [9] Alligné S., Nicolet C., Tsujimoto Y., Avellan F, Cavitation surge modelling in Francis turbine draft tube *J. of Hydraulic Research*. 2014, **52** (3).
- [10] Landry C., Favrel A., Müller A., Nicolet C., Avellan F., Experimental identification of the local wave speed and the second viscosity in cavitating draft tube flow *J. of Hydraulic Research* 2014.
- [11] Nicolet C., Herou J.-J., Greiveldinger B., Allenbach P., Simond J.-J., Avellan F, Methodology for Risk Assessment of Part load resonance in Francis turbine power plant. In Proc. of the IAHR Int. Meeting of WG on Cavitation and Dynamic Problems in Hydraulic Machinery and Systems, Barcelona, 2006.
- [12] Alligné S., Landry C., Favrel A., Nicolet C., Avellan, F., Francis turbine draft tube modelling for prediction of pressure fluctuations on prototype. In Proc. of 9<sup>th</sup> International Symposium on Cavitation, 2015.

## Acknowledgments

The research leading to the results published in this paper is part of the HYPERBOLE research project, granted by the European Commission (ERC/FP7-ENERGY-2013-1-Grant 608532). The authors would like to thank BC Hydro for making available the reduced scale model and the prototype for validation, in particular Dany Burggraeve and Jacob Iosfin. Finally, parameters of the electrical model have been provided by Mr. Johann Hell from ANDRITZ Hydro who authors would like to thank.